Range image accuracy improvement by acquisition planning

F. Prieto *(1,2)*, H.T. Redarce *(1)*, R. Lepage *(2)* and P. Boulanger *(3)*

1. Laboratoire d'Automatique Industrielle,
Institut Nationale des Sciences Appliquées
20 avenue Albert Einstein, 69621 Villeurbanne, France
redarce@lai.insa-lyon.fr

2. Laboratoire d'Imagerie, de Vision et d'Intelligence Artificielle,
Ecole de Technologie Supérieure
1100 rue Notre-Dame Ouest, Montréal, Québec, H3C 1K3, Canada
lepage@livia.etsmtl.ca

3. Institute for Information Technology,
National Research Council of Canada
Montreal road, building M-50, Ottawa, Ontario, K1A 0R6, Canada
boulanger@iit.nrc.ca

Abstract

The recent requirement for increased speed in the design and manufacturing of new products led to a rapid evolution of the technics for fast production (rapid prototyping, machining at high speed, etc.). But a significant component did not follow this evolution, that is the dimensional and functional checking process, which is most of the time carried out in a traditional way. The use of range sensor allows very significant improvement in acquisition speed but does not equal the accuracy obtained with a coordinate measuring machine. In order to obtain a quality control close to that obtained in metrology, we suggest to improve the accuracy of the depth measurements by following an acquisition strategy. We propose in this paper such a strategy to automatically produce a sensing plan for completely and precisely acquiring the geometry of a surface or of a complete piece whenever possible. The system requires the exact position and orientation of the part and its CAD model in IGES format. There is no limitation regarding the shape of the part to be digitized. A Biris sensor was used, and for this sensor, the precision of the 3D measured points is function of the distance and of the incident angle with which the laser beam reaches the surface. Our strategy guaranties that the viewpoint found meets the best precision conditions in the scanning process.

1 Introduction

The increased production rate of manufactured objects showing complex surfaces, either for functional reasons or by design, and the technological developments in manufacturing tools create a need for automatic inspection of complex parts. This type of control requires a very accurate geometrical definition of the inspected object, a large number of acquisition points with sufficient accuracy, and clearly defined rules for the inspection of these surfaces.

The use of three-dimensional measuring machines and recent progress in laser sensors combining measurement accuracy and fast acquisition speed allow to obtain many 3D measurements. These accurate 3D points form an explicit description of object surfaces. In addition, knowledge of the corresponding CAD model provides an exact and complete description of the geometry of the object under inspection. We develop a method for automatic inspection of parts containing complex surfaces, running from their CAD model (in IGES format) and 3D data output provided by a telemetric sensor fixed to a coordinate measuring machine. The quality of the results depends almost exclusively on the precision of measurements.

At present, it is near to impossible to compare the accuracy obtained with a coordinate measuring machine equipped with a contact sensor (lower than the micron) and those delivered by a measuring machine equipped with a laser range finder (about 25 micron at best). If one wants to take advantage from the speed of acquisition obtained with a contactless sensor to make systematic dimensional check of complex parts, it is necessary to attain the best precision of the depth images obtained with a range finder.

3D sensors, delivering information about the geometry of the object, all operate generally according to a common principle: emission of a laser beam (incidental ray), generally from a laser diode, followed by the analysis of the reflected ray [2, 3]. From this analysis, we obtain the spatial position of each swept point (x, y, z), relative to

the reference frame of the sensor, and also for certain sensors the luminance information. The optics laws dictate that the laser ray be normal to the surface if we want that the reflected ray has a maximum of energy.

In order to meet this constraint of perpendicularity, we propose digitizing the object by following strategies allowing to keep the laser beam as normal as possible to the queried surface. Moreover, the sensor used to carry out our experiments (a Biris laser sensor) have the property of increased precision when it is closer to the object, the minimal distance corresponding to its depth of field. Therefore, we have developed a constrained digitalization technique allowing at the same time to keep the sensor as normal as possible to the surface, while obeying a criterion of accuracy defined by the operator and chosen to avoid occlusions. This planning of trajectory is based on a knowledge *a priori* of the object with the use of a CAD data base containing all the information on the object from its design phase.

We present in this paper this acquisition planning strategy as well as results obtained on computer-generated images and real data.

2 Review of literature

The majority of work carried out in the field of sensor position planning is aimed at finding the best views to scan the object without missing regions, and with a minimum number of views. It is usually considered that the environment is unknown, that no information on the type of object is available, neither its position nor its orientation. On this subject we can quote the article by Tarabanis et al. [10], which is "a survey" of the question, where the problem is tackled from the point of view of the depth images (3D) and of the illuminance images (2D). In the case of the 2D images we can quote work of Cowan and Kovesi [5] and also Ben Amar et al. and Redarce et al. [1, 9].

Tarabanis et al. [11] developed a model-based sensor planning system. The Machine Vision Planner (MVP) automatically computes vision sensor parameter values that satisfy several sensor constraints such as detectability, visibility and field of view. Inputs to the MVP system are: the object geometry information from a CAD database as well as camera and lens models. Outputs are the camera position and setting values for which features of interest of polyhedral objects are visible, contained entirely in the sensor field of view, in focus and resolvable by the given specifications of the sensor. This system works with 2D image obtained from a CCD camera.

Truco et al. [13, 12] reported a general automatic sensor planning system (GASP) designed to compute optimal positions for inspection tasks, using a known imaging sensor (like a 3D range sensor) and feature-based object models. GASP exploits a feature inspection representation (FIR) which outputs off-line the explicit solution for the sensor-positioning problem. Viewpoint is defined optimally as a function of feature visibility and measurement reliability. GASP computes visibility with an approximate model; the reliability of inspection depends on the physical sensors used and on the processing software. Truco et al. demonstrate a complete inspection session involving 3D object positioning, optimal sensor position, and feature measurement from the optimal viewpoint.

Newman and Jain [7] developed a system that permits the detection of defects in range images of castings. This system uses CAD model information for surface classification and inspection. Authors assert there are several advantages for the use of range images in inspection. For example: the accuracy of depth measurement and the insensitivity to ambient light that usually allows the objects to be extracted more easily from their background, and most important, range images explicitly represent surface information. In this paper however, there is no information about the strategies for the scanner positioning. The authors show the interest for the use of the CAD data base in order to carry out the control task. Moreover, they show the weakness of the current CAD systems to make automatic check.

We have worked for several years on measurement control by comparison of CAD models and range images [6, 8]. The size of the defects which can be detected depends in a very significant way on the sensor accuracy. Therefore we seek to improve the accuracy by building strategies for images acquisition.

3 The 3D laser camera

Our work is based on the use of a Biris sensor[1], but may be easily extended to other 3D sensor. The optical principle of this sensor[2] is based on a combination of optical triangulation and the use of a double aperture mask in the iris plane of the camera lens. While the auto-synchronized technology provides high accuracy and high resolution 3D images, the basic objective of this technology was to provide a low cost, robust solution to industrial 3D imaging.

A double aperture mask is introduced in front of a conventional camera lens. A single target point P illuminated on the object surface creates two distinct intensity peaks P_1 and P_2 on the camera CCD sensor. The geometric position of the peaks P_1 and P_2 is a function of the

1. Designed by NRCC (National Research Council of Canada) and manufactured and marketed by Vitana company.
2. The explanation of optical principle can be obtained from NRCC web site at http://www.vit.iit.nrc.ca/.

distance from the camera to the target point *P: Distance = f* (P_1,P_2). The intensity from the target point *P* is the sum of the intensities at P_1 and P_2: *Intensity* = $I_{P1} + I_{P2}$.

The scanning of the target surface by the sensor results in the output of 3D points (*x, y, z*) and their illuminance *(I)* at the surface. The Biris sensor scans surface line by line at a rate of 256 points/line, the resolution being a function of the length of this line, and therefore of the distance separating the sensor from the object. The field of view angle α is 23 degrees and the minimal distance (d_{min}) object/sensor is 160 millimeters. In order to scan the whole part, the Biris sensor is fixed on a robot arm to locate the camera anywhere in the workspace, and an additional rotation (sweep angle β) carries out the sweeping of a surface.

4 The 3D acquisition strategy

The main goal of this work is to improve the measurement precision of a part with the aid of a 3D points acquisition strategy. An acquisition strategy consists in computing the set *X* of *viewpoints* x^i in order to obtain a complete and optimal 3D image of the part. An optimal 3D image is a 3D cloud issued by the scanning process in the best accuracy conditions. The resulting 3D image could be used in inspection task for instance. In inspection task, we are most of the time interested in verifying the specification of just some few surfaces. Our strategy is to find the collection of viewpoints for each digitized surface. If one wants to digitize the whole part, we just have to add the complete assemblies *X* of all the surfaces in the piece.

We define a *viewpoint* as a set of 7 parameters $x^i=\{x_1 \dots x_7\}^i$, where three *position parameters* (*x, y, z*) define the spatial position of the camera relative to the coordinate system of the part, three *orientation parameters* (ϕ, θ, ψ) define the direction of the laser beam, and one parameter β specifies the angle of the controlled sweep. We do not consider optical parameters because the laser camera is previously calibrated. The set **X** of viewpoints x^i is defined $\mathbf{X}= \{x^1\ x^2 \dots x^n\}$, where *n* is the minimum number of viewpoints to digitize a surface or the whole piece.

The system requirements are: a knowledge of the exact position and orientation of the part and the CAD model of the part in IGES format. We use a registration process to determine the placement of the part, as implemented by Moron [6] and which relies on the well-known work of Besl and McKay [4]. This process registers an unordered cloud of 3D points of the part with its CAD model. The CAD model is used not only in the registration process, but also in the search of viewpoints to solve the occlusion problems.

The accuracy of a measured point in the digitalization process using a Biris 3D laser camera depends on the scanning distance and on the angle of incidence of the laser beam on the surface. The range specification of the Biris sensor states the near and far range of view planes as 165mm and 645mm respectively, the measured points being then more accurate when the camera is located near the part. The ideal incident angle is 90 degrees, that is the more the angle of incidence of the laser ray is near to the normal surface direction, the more the measured points are accurate. Our strategy searches for viewpoints to digitize the part with the best conditions for precision.

The viewpoint issues of our strategy are that they can be reached by the camera mechanical support and are occlusion free. A surface is occluded for a specific viewpoint if the laser beam is intersected by any object before reaching the target surface. The system works with both simple and complex surfaces. The only geometric constraint imposed to the parts to be digitized is that they are completely contained in the work space of the camera. Figure 1 shows a viewpoint with all of its parameters.

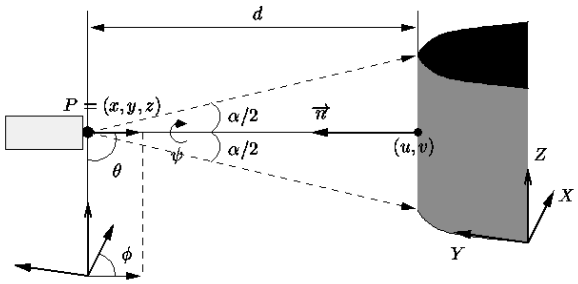

Figure 1. Parameters of a viewpoint.

4.1 The CAD model

The system includes a CAD model of the inspected part in IGES format. The IGES file contains the exact representation of the part using NURBS (Non Uniform Rational B-Splines) surfaces parameters. Those surface components are used to search the viewpoints and to solve the collision and occlusion problems. We first create a 2D bitmap of each surface to find the placement of the viewpoints on the surface. The normal direction of these points is computed using the parameters of the NURBS surface. In order to solve the occlusion problem a *3D surface model* composed of voxels is created using all the NURBS surfaces of the part.

A NURBS surface of order *p* in the parametric direction *u* and of order *q* in parametric direction *v* is defined by the following equation:

$$\vec{s}(u,v) = \frac{\sum_{i=0}^{n}\sum_{j=0}^{m} N_{i,p}(u)N_{j,q}(v)w_{i,j}P_{i,j}}{\sum_{i=0}^{n}\sum_{j=0}^{m} N_{i,p}(u)N_{j,q}(v)w_{i,j}}$$

where n and m are the number of control points in the parametric direction u and v respectively, $P_{i,j}$ are the control points, $w_{i,j}$ the weight associated to the control point $P_{i,j}$, $N_{i,p}$ (or $N_{j,q}$) the B-Spline base functions defined by the following recurrent formula:

$$N_{i,p}(u) = \frac{u-u_{i-1}}{u_{i+p-1}-u_{i-1}}N_{i,p-1}(u) + \frac{u_{i+p}-u}{u_{i+p}-u_i}N_{i+1,p-1}(u)$$

$$N_{i,0}(u) = \begin{cases} 1 & \text{if } u_{i-1} \le u \le u_i \\ 0 & elsewhere \end{cases}$$

where u_i, v_j are the inner knots belonging to the knot vectors of the NURBS surface, u_i in $[u_0,u_1]$ and v_j in $[v_0,v_1]$.

Let $P(u, v)$ be a 3D surface representation of a part, defined by the union of its N parametric surfaces:

$$P(u,v) = \begin{pmatrix} \sum_{i=1}^{N} \vec{s}_i(u,v) \\ \sum_{i=1}^{N} (X_i(u,v), Y_i(u,v), Z_i(u,v)) \end{pmatrix} = P_{(x,y,z)}$$

Let $P_D(x, y, z)$ be the *3D surface model* of the piece $P(u, v)$, and defined by:

$$P_D(x,y,z) = \sum_{i=1}^{Ni}\sum_{j=1}^{Nj}\sum_{k=1}^{Nk} (Inf(X_i(u,v)), Inf(Y_j(u,v)), Inf(Z_k(u,v))) = V_{ijk}(x,y,z)$$

where $Inf(X(u, v))$ is the biggest integer inferior or equal to $X(u, v)$, and V_{ijk} defines a *voxel* as: $x^i \le x < x^i + 1, y^j \le y < y^j + 1$, and $z^k \le z < z^k + 1$. If we extend the concept of a two-dimensional binary bitmap, where each pixel (i, j) can take just one of two values, each voxel (i, j, k) in the 3D space can take one of two values: *0* (unoccupied) or *1* (occupied). An occupied voxel contains some portion of any of the surfaces that comprise the piece. The *3D surface model* P_D is the addition of all occupied voxels. Clearly, $P(x,y,z) \subseteq P_D(x,y,z)$. The importance of this *3D surface model* in the solution of the occlusion problem will be clarified later

4.2 Viewpoints and accuracy

The accuracy of measured points by a Biris camera is a function of the distance d between the camera and the part being digitized and the incidence angle of the laser beam. The area of the surface to be digitized from a specific viewpoint depends on the distance d, the sweep angle β, and the field of view α of the scanner. In most cases the field of view α of the camera is fixed. In fact, the portion of surface digitized from a specified viewpoint is defined by the rectangle $R=ab$, where a is the line formed by the laser ray projection on the surface and equals to $a = 2 \cdot d \cdot tan\alpha/2$, and b is the sweeping line of the laser ray from robot arm motion in a direction perpendicular to the laser line on the part, and defined by $b = 2 \cdot d \cdot tan\beta/2$.

It should be obvious that there is a relationship between the minimal number of viewpoints needed to digitize a surface (or the complete piece) and the accuracy of this measurement. For example, if we place the camera away from the part and allow a large sweep angle, we need just a few viewpoints for the whole digitalization, but the accuracy is poor. Our work mainly is thus to look for accuracy improvement in the measurement of 3D points, and to use them in tasks like inspection. We developed an algorithm that searches for the minimal number of viewpoints necessary to digitize a surface, constraining the distance d of the camera placement and the sweep angle β. The field of view α of the camera is settled from the scanner specifications. The range of the distance d and of the sweep angle β are: $d_i \le d \le d_f$, and $\beta_i \le \beta \le \beta_f$ respectively. Those parameters are obtained from the camera and mechanical support specifications. In order to test our algorithm and to experiment with our collection of manufactured parts (most included in a volume of $100mm \times 100mm \times 100mm$ }, we have settled parameters as: d_i=100mm, d_f=120mm, β_i=10°, β_f=15° and α=15°.

Our algorithm uses a 2D bitmap obtained from the NURBS surface definition, and compute the best orientation of placement (in the parametric directions), and the number of *digitizing rectangles* required for the whole digitalization of the surface. Initially, the best direction for the laser sweep ray is found (sweep ray is specified by the scanner's field of view α). The best direction is defined as the direction where the variation of the incidence angle (of the laser ray) for a complete sweep is the smallest. To that end, the direction is found where the surface touched by the laser beam has the smallest curvature. This algorithm has to work with any kind of surfaces (simple and complex ones), therefore the selection of a good direction is a very important criteria. Figure 2 shows the number and placement of the *digitizing rectangles* obtained for a curved surfaces in the two parametric directions. Solution (a) needs just two viewpoints compared to the five needed in solution (b), but as the variation of the incident angle is larger in solution (a) (about 180°), than in solution (b) (about 45°), the solution retained is the second one. It should be noted that solution (a) optimizes the distance d

from the digitized surface but relax the incident angle constraint, while the solution (b) relax the distance constraint but restricts the allowed incident angle range.

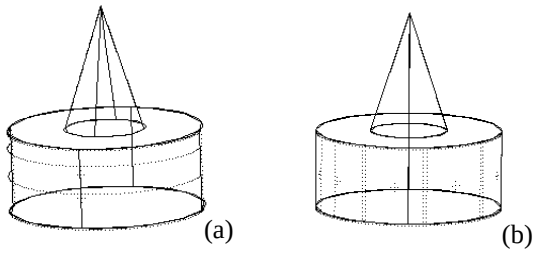

Figure 2. Incident angle variation on a curved surface

In Figure 3, we look at the solution for a flat surface. Figure 3(b) shows the number of required viewpoints (7) as the emphasis is put on minimizing the distance *d*, while figure 3(a) minimizes the variation of angle β and necessitates 5 viewpoints. For this example, since the variation of incident angle curvature is similar in the two parametric directions, the retained solution is (a) because it needs less viewpoints.

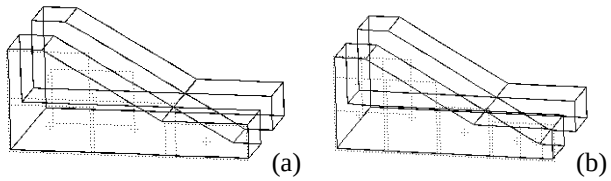

Figure 3. Finding the minimum number of viewpoint

Looking at figure 3(a) or 3(b), we conclude that the solution found is not optimal. In fact there are some viewpoints defined for digitizing just a small region of surface. The algorithm further optimizes the number of viewpoints by eliminating viewpoints associated with too small regions (where the digitized area is usually less than 25% of the biggest one). The remaining viewpoints are modified, either in the their sweep angle β and/or in their distance *d*, to include these small regions.

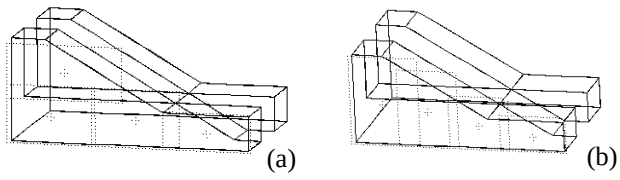

Figure 4. Optimal solution by changing β and *d* parameters

Figure 4 shows an optimized solution for the piece shown in figure 3. In both solutions, the number of viewpoints have been reduced to four, but solution (a) is retained because it needs to modify just one viewpoint. We recall that the viewpoints are defined to have the best accuracy, and any modification of β or *d* parameters produces a decrease in the accuracy of measured points.

4.3 Finding the normal direction

To achieve the definition of a viewpoint, we need to find its position and orientation in the space. For that purpose, we compute the normal direction of the viewpoints obtained in the previous section. For a point *(u, v)*, on the parametric surface $\vec{s}$, the normal direction is computed by using:

$$\vec{n} = \frac{\frac{\partial}{\partial u}\vec{s}(u,v) \times \frac{\partial}{\partial v}\vec{s}(u,v)}{\left\| \frac{\partial}{\partial u}\vec{s}(u,v) \times \frac{\partial}{\partial v}\vec{s}(u,v) \right\|^2}$$

with $\frac{\partial}{\partial u}\vec{s}(u,v) = \frac{AB - CD}{E^2}$ and $\frac{\partial}{\partial v}\vec{s}(u,v) = \frac{FB - GD}{E^2}$

where

$$A = \sum_{i=0}^{n}\sum_{j=0}^{m}\left(\frac{\partial}{\partial u}N_{i,p}(u)\right)N_{j,q}(v)w_{i,j}P_{i,j} \quad ,$$

$$B = \sum_{i=0}^{n}\sum_{j=0}^{m}N_{i,p}(u)N_{j,q}(v)w_{i,j},$$

$$C = \sum_{i=0}^{n}\sum_{j=0}^{m}N_{i,p}(u)N_{j,q}(v)w_{i,j}P_{i,j}$$

$$D = \sum_{i=0}^{n}\sum_{j=0}^{m}\left(\frac{\partial}{\partial u}N_{i,p}(u)\right)N_{j,q}(v)w_{i,j}$$

$$E = \sum_{i=0}^{n}\sum_{j=0}^{m}N_{i,p}(u)N_{j,q}(v)w_{i,j}$$

$$F = \sum_{i=0}^{n}\sum_{j=0}^{m}N_{i,p}(u)\left(\frac{\partial}{\partial v}N_{j,q}(v)\right)w_{i,j}P_{i,j}$$

$$G = \sum_{i=0}^{n}\sum_{j=0}^{m}N_{i,p}(u)\left(\frac{\partial}{\partial v}N_{j,q}(v)\right)w_{i,j}$$

$$\frac{\partial}{\partial u}N_{i,p}(u) = \frac{p}{u_{i+p-1}-u_{i-1}}N_{i,p-1}(u) - \frac{p}{u_{i+p}-u_i}N_{i+1,p-1}(u) \quad \text{and}$$

$$\frac{\partial}{\partial v}N_{j,q}(v) = \frac{q}{u_{j+q-1}-u_{j-1}}N_{j,q-1}(v) - \frac{q}{u_{j+q}-u_j}N_{j+1,l-1}(v)$$

In figure 5, we show the viewpoints found by using our strategy for two pieces. In Figure 5(a), we illustrate the viewpoint's orientation change when we digitize a complex surface. In figure 5(b), we remark the viewpoint distance variation as a function of the area to digitize.

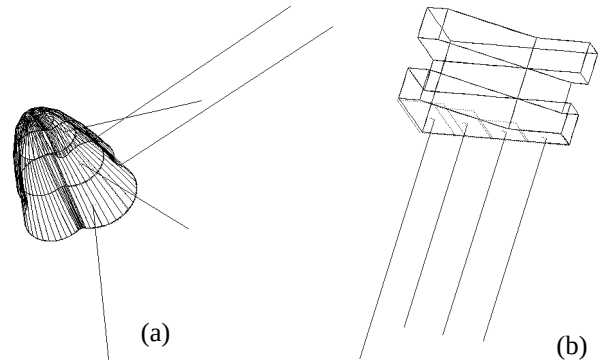

Figure 5. Normal directions to the surface

4.4 The occlusion problem

Until now, the viewpoints are found for the best precision condition. The next step in our strategy is to verify that the viewpoint position is reachable and that it is free from occlusion problem. For the reachability, we suppose that the part is in the center of a sphere, and that the viewpoints out of this sphere can be reached by the mechanical support of the camera. As the part is modeled according to a *3D surface model* composed of voxels, we can delimit the workspace by adding the model of other objects present in the scene. For occlusion verification, we insure that the laser beam coming from the viewpoint position to the target surface is not intersected by any object. When an occlusion problem is detected, the system seek for a new viewpoint by moving the old viewpoint in the parametric directions of the surface. The new viewpoint will optimize the accuracy constraints by ensuring the visibility of the region to be digitized. Figure 6 shows the digitalization viewpoints found for some surfaces that initially presented an occlusion problem.

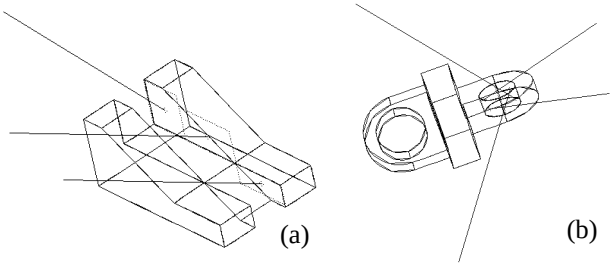

Figure 6. Viewpoints without occlusion problem

5 Sensor planning simulation

In the last section, we have described our strategy for automatically setting a sensor position planning for completely and precisely acquiring the geometry of a surface or a part whenever possible. In this section, we present results of a sensing planning for the complete digitalization of some parts. To facilitate testing, we have implemented an algorithm using the CAD model of the part to artificially generate range images of the parts from any viewpoint.

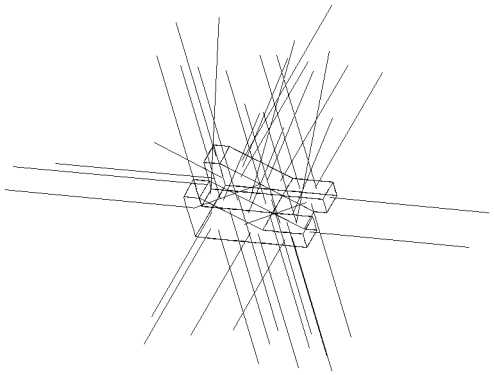

Figure 7(a). Sensing planing of a synthesized range image

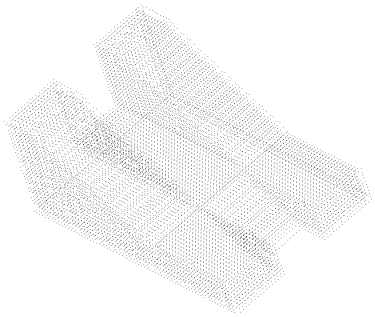

Figure 7(b). Synthesized range image

In Figure 7(a) we look at the sensing planning for a complete digitalization of a surface made of flat surfaces. Some surfaces of the part exhibited occlusion problem that was resolved. For a complete scanning, the strategy has found 42 viewpoints. In Figure 7(b), we show the synthesized range image generated by using the 42 viewpoints, and we can see that there are no missing regions of the part.

In figure 8(a), we illustrate the sensing planning for the complete digitalization of a complex part. For the whole scanning, the strategy has found 44 viewpoints. In figure 8(b) and 8(c), we show the synthesized range image generated by using the 44 viewpoints, resulting in no missing regions neither. For this part we remark that the

position variation of viewpoints remains always near to the normal direction of the surfaces.

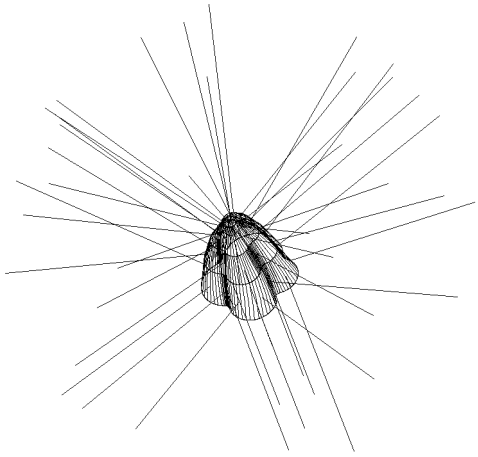

Figure 8(a). Sensing planning of an synthesized range ima for a complex part.

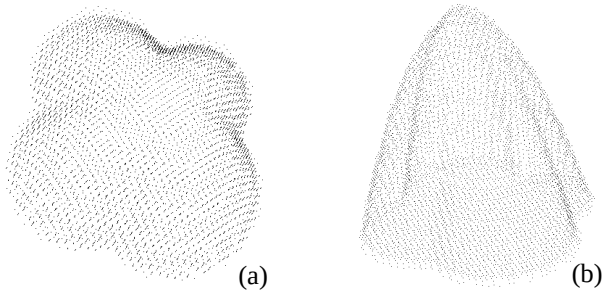

(a) (b)

Figure 8. synthesized range image

6 Practical results

In order to verify our hypotheses for accuracy improvement of the 3D points cloud by optimizing the camera placement, we have evaluated the accuracy of our measurements. We have realized 128 measurements in different positions of distance and orientation of the laser sensor with respect to a reference surface.

In figure 9 we present the variance (in mm^2) in the axis of the projected beam versus the distance (in mm) from the camera to the surface. From Figure 9, we can conclude that in spite of small oscillations, the variance has a smaller dispersion when the camera is near to the surface for distance up to 215 mm.

In figure 10 we present the variance (in mm^2) in the laser propagation axis versus the incident angle (in degrees) the laser beam reaches the surface. The incident angle is measured in the same direction as the laser beam sweep. From figure 10 we observed that the smaller value of dispersion is produced for an incident angle range between 15 and 30 degrees, but not in the vicinity of 0^o as expected. This result is due to the inclination between the CCD sensor and the laser head in the Biris camera in order to produce the optical triangulation. A correction in the orientation parameter for our planning strategy had to be applied.

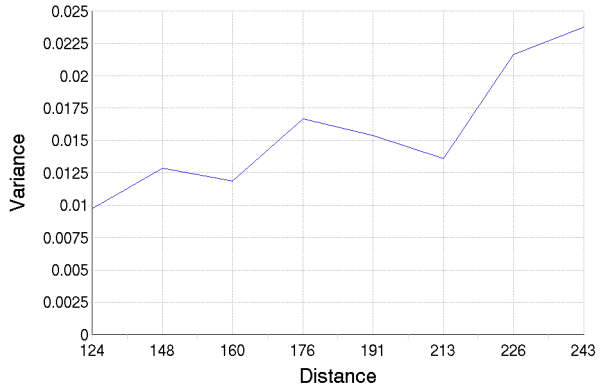

Figure 9. Variance versus distance

Figure 10. Variance versus incident angle in the direction of the laser sweep.

In figure 11 we present the variance (in mm^2) in the axis of the beam projection versus the incident angle (in degrees). Here, the incident angle is measured in a perpendicular direction from the laser beam sweep. From figure 11 we can conclude that the dispersion is smaller when the incident angle is near to zero, or normal to the surface. For an incident angle larger than 40 degrees, the dispersion becomes most important.

These results confirm that we can improve the accuracy of the data acquisition process by following the criterions which we defined (normal direction, distance). If these criterions cannot be met, because of occlusions for example, it will be always possible to assign a weighting

factor to the acquired points, depending on the acquisition conditions.

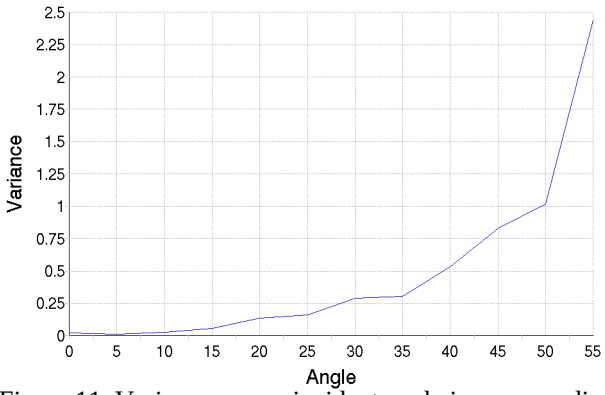

Figure 11. Variance versus incident angle in a perpendicular direction to the laser sweep.

7 Conclusion

We have presented an automated acquisition planning strategy to improve the accuracy of the measured 3D points. The strategy computes a set of viewpoints in order to obtain a complete and accurate image of the part or selected surfaces in the part. The viewpoints are constrained to have the best precision conditions in the scanning process. For a Biris sensor, those constraints are the distance to the part and the orientation of the incident laser beam. The strategy can be easily adapted to use other kind of range sensors and mechanical supports.

The system does not have any limitation in the geometry of parts to be scanned, meaning that it works as well with simple or complex parts. In order to use the 3D measured points in tasks like inspection, the strategy permits to digitize only the surfaces of interest.

At present, the sequence of viewpoints for the scanning process is computed without any special computer configuration. Even if the acquisition planning is made off lines, it will be necessary to implement a method to optimally lay out the viewpoints in order to reduce the scanning time.

8 References

[1] Ben Amar, C., Perrin, S., Redarce, H.T., and Jutard, A. "Intégration d'un module vision dans un système de CAO-robotique: modélisation et aide au placement de capteurs", *Congrès international de génie industriel la productivité dans un monde sans frontiéres*, Montréal, Canada, 1995, Octobre 18-20, pp. 725-734.

[2] Beraldin, J.-A., Cournoyer, L., Rioux, M., Blais, F., El-Hakim, S.F., and Godin, G. "Object model creation from multiple range images: acquisition, calibration, model building and verification". *Proceedings of the International Conference on Recent Advances in 3-D Digital Imaging and Modeling*, Ottawa, Ont., 1997, May 12-15, pp. 326-333.

[3] Beraldin, J.-A., El-Hakim, S.F., and Blais, F. "Performance evaluation of three active vision systems built at the NRC". *Proceedings of the Conference on Optical 3-D Measurement Techniques*, Vienna, Austria, 1995, October 2-4, pp. 352-362.

[4] Besl, P.J. and McKay, N.D. "A method for registration of 3-D shapes", *IEEE Transactions on Pattern Analysis and Machine Intelligence*, vol. 14, No 2, 1992, February, pp. 239-256.

[5] Cowan, C.K. and Kovesi, P.D. "Automatic sensor placement from vision-task requirements", *IEEE Transactions on Pattern Analysis and Machine Intelligence*, vol. 10, No 5, 1988, May, pp. 407-416.

[6] Moron, V., Boulanger, P., Masuda, P. and Redarce, H.T. "Automatic inspection of industrial parts using 3-D optical range sensor", *SPIE Proceedings, Videometrics IV*, vol. 2598, 1995, pp. 315-325.

[7] Newman, T.S., and Jain, A.K. "A system for 3D CAD-based inspection using range images", *Pattern Recognition*, vol. 28, No10, 1995, pp. 1555-1574.

[8] Prieto, F., Redarce, H.T., Lepage, R., and Boulanger, P. "Visual system for the fast and automated inspection of 3D parts", *7th European Conference on Rapid Prototyping*, Paris, France, 1998, November 19-20, pp. 273-285.

[9] Redarce, H.T., Lucas, Y., Ben Amar, C., and Perrin, S. "An integrated approach for programming vision inspection cells", *International Journal of Computer Integrated Manufacturing Systems*, vol. 8, No 4, 1995, April, pp. 298-311.

[10] Tarabanis, K.A., Allen, P.K., and Tsai, R.Y. "A survey of sensor planning in computer vision", *IEEE Transactions on Robotics and Automation*, vol. 11, No 1, 1995, February, pp. 86-104.

[11] Tarabanis, K.A., Tsai, R.Y., and Allen, P.K. "The MVP sensor planning system for robotic vision tasks", *IEEE Transactions on Robotics and Automation*, vol. 11, No 1, 1995, February, pp. 72-85.

[12] Trucco, E., Diprima, M., and Roberto, V. "Visibility scripts for active feature-based inspection", *Pattern Recognition Letters*, vol. 15, 1994, pp. 1151-1164.

[13] Trucco, E., Umasuthan, M., Wallace, A. M., and Roberto, V. "Model-based planning of optimal sensor placements for inspection", *IEEE Transactions on Robotics and Automation*, vol. 13, No 2, 1997, April, pp. 182-194.